

PROCEEDINGS OF SPIE

[SPIDigitalLibrary.org/conference-proceedings-of-spie](https://spiedigitallibrary.org/conference-proceedings-of-spie)

ORCAS – Orbiting Configurable Artificial Star Mission Architecture

Eliad Peretz, Christine Hamilton, John Mather, Lucas Pabarcus, Kevin Hall, et al.

Eliad Peretz, Christine Hamilton, John C. Mather, Lucas Pabarcus, Kevin Hall, Adam Michaels, Robert Pritchett, Wayne Yu, Peter Wizinowich, Eric Golliher, "ORCAS – Orbiting Configurable Artificial Star Mission Architecture," Proc. SPIE 11819, UV/Optical/IR Space Telescopes and Instruments: Innovative Technologies and Concepts X, 1181905 (20 August 2021); doi: 10.1117/12.2594789

SPIE.

Event: SPIE Optical Engineering + Applications, 2021, San Diego, California, United States

ORCAS – Orbiting Configurable Artificial Star Mission Architecture

Eliad Peretz^a, Christine Hamilton^a, John C. Mather^a, Lucas Pabarcus^a, Kevin Hall^b, Adam Michaels^a, Robert Pritchett^a, Wayne Yu^a, Peter Wizinowich^c, Eric Golliher¹

^aNASA Goddard Space Flight Center, Greenbelt, MD 20771, USA

^bUniversity of Maryland, Department of Astronomy, 7950 Baltimore Avenue, College Park, MD, USA, 20742

^cW. M. Keck Observatory, Mauna Kea, HI 96781

Abstract.

In this paper, we establish the mission operation concept for the Orbiting Configurable Artificial Star mission, a hybrid space-ground observatory, which aims to enable ground observations of near-diffraction limited resolution and exquisite sensitivity. We present the mission requirements, introduce a potential orbit solution that can meet them, detail the concrete operational steps to be taken to enable such observations, and develop a mission planning tool which generates a mission schedule that meets all mission requirements and can be altered in real time in the case of disruptions to the mission. Finally, we show the the mission could enable 300 adaptive optics and 1500 flux calibration observations throughout its lifetime.

Keywords: Adaptive Optics, Extremely Large Telescopes, Numerical Simulations, Optimization, Mission Architecture.

*Eliad Peretz, eliad.peretz@nasa.gov

1 Introduction

The Orbiting Configurable Artificial Star (ORCAS) mission would be a hybrid space and ground observatory which would allow ground telescopes to greatly increase their angular resolution, sensitivity, and science target accessibility by using a laser guide star to improve Adaptive Optics (AO).¹⁻³ The ORCAS mission explicitly addresses two of the top three priorities of the 2010 Decadal Survey: “Cosmic Dawn: Searching for the First Stars, Galaxies, and Black Holes,” and “Physics of the Universe: Understanding Scientific Principles.”⁴ One of the great mysteries is the existence and growth of super-massive black holes through the merger of protogalaxies and the accretion of gas and stars; our ability to solve this mystery is limited by current angular resolution and sensitivity.⁵ The cosmic dark energy is likewise a mystery that has only grown deeper as measurements improve and disagreements appear. Photometric calibration is currently one of the largest error terms in dark energy measurements. As shown in Figure 1, ORCAS explores a new parameter regime in angular resolution and sensitivity, allowing for huge potential advances for these questions.⁶⁻⁹

ORCAS would enable observations of many science cases, including Active Galactic Nuclei, Supernovae, the high redshift universe, the solar system, exoplanets, and flux calibration. All these science cases could see large advances from the new angular resolution and sensitivity regimes enabled by ORCAS.

The mission would consist of two parts: a satellite with both a laser and a flux calibrator payload, and the observatory itself. An illustration of the mission concept can be seen in Figure 2. For an AO observation, the ORCAS spacecraft would need to inertially align within arcseconds of the pointing direction of an observatory on Earth and the observation target. It would then need to stay within the ground telescope’s field of view for the entire observation time, providing the laser signal to the observatory. A flux calibration observation can be done based on a streak of the ORCAS spacecraft, so the observation time constraint is much less strict.

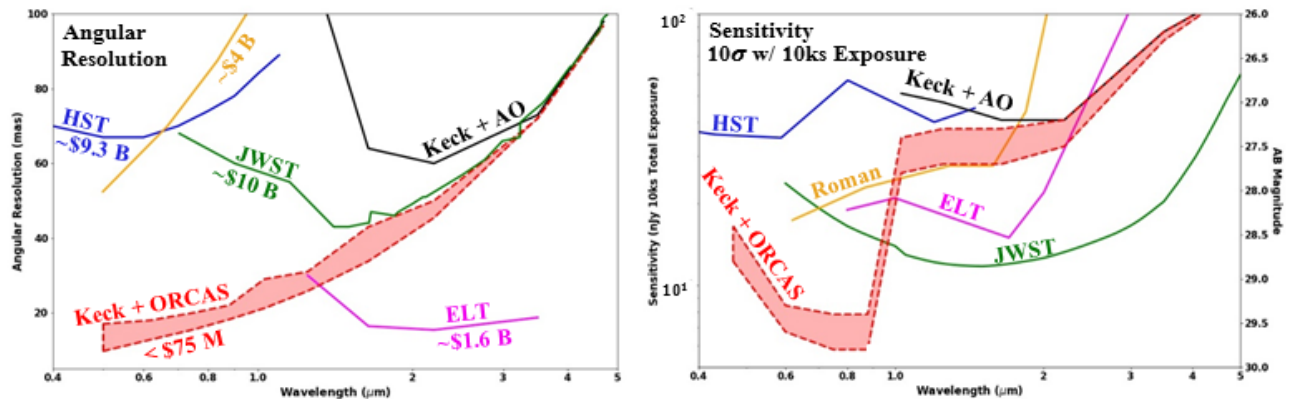


Fig 1 ORCAS performance complements other future observatories both in space and on the ground. A: The angular resolution as a function of wavelength, B: the sensitivity as a function of wavelength (for SNR = 5 in 10000 s). Note that ORCAS enables different exposure times based on the target declination.

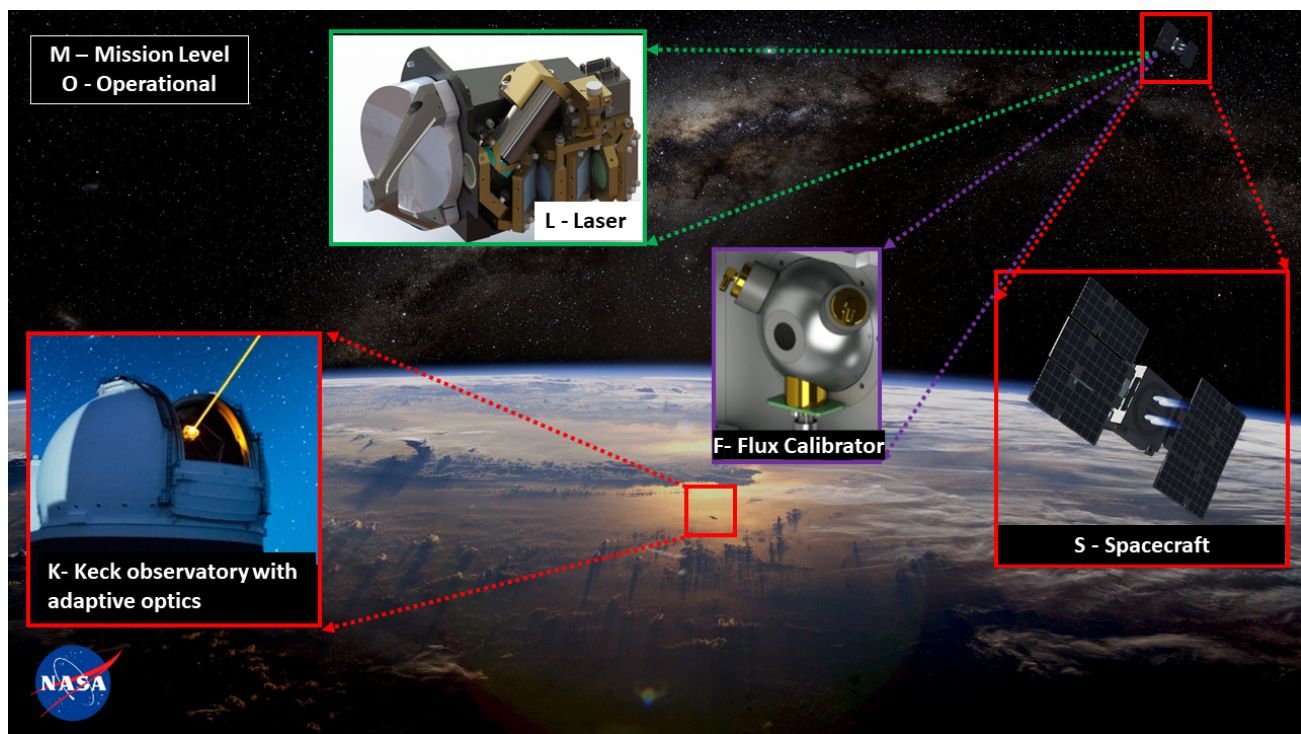


Fig 2 The major ORCAS mission components. Labels for each component corresponds to the engineering requirements traceability matrix seen in Table 1.

This paper outlines the proposed mission architecture and mission planning tool for ORCAS. The overall mission requirements are described in Section 2, followed by the observational requirements in Section 3. We then describe the highly elliptical orbit which can meet the observational requirements for a single observation in Section 4, along with the proposed observation sequences and mission lifetime schedule. Then, the methods for developing the ORCAS mission planning tool, which optimizes the order of observation targets to be viewed over the mission lifetime, are given in Section 5. The

results of our mission planning tool are given in Section 6, which includes a detailed example schedule for ORCAS observations. Finally, Section 7 discusses these results and future work that should be done on the topic.

2 Mission Requirements

The mission engineering requirements have been defined by the science teams working with ORCAS to ensure the mission is able to meet the goals for each of six science cases. These requirements are outlined in Table 1. Each requirement is labeled for traceability. The first number in the prefix corresponds to the science case, where the science cases are **1)** Exoplanets, **2)** Solar System, **3)** Supernovae, **4)** Active Galactic Nuclei, **5)** High Redshift Universe, and **6)** Flux Calibration. The letter corresponds to the requirement component as defined in Figure 2, where the components are **M)** Mission level, **O)** Operational, **L)** Laser, **K)** W. M. Keck Observatory (WMKO), **F)** Flux Calibrator, **S)** Spacecraft. Finally, the last number indicates the identifying number of the requirement. For example, requirement 1.M.1 identifies itself as a requirement for the Exoplanet science case defined by the Mission Level, and it is the first such requirement. More information about the laser payload system used for ORCAS can be found in a paper our team has written on that topic.¹⁰

Table 1 Engineering Requirement Traceability Matrix. Each bold numeral in the prefix corresponds to its respective ORCAS science case. If multiple science cases have an identical requirement, a single row will be filled. The letter corresponds to the mission component as defined in Figure 2.

Requirement Traceability Matrix			
Prefix	Parameter	Requirement	Expected Performance
1 .M.1	Observations	30 Targets, 2 observations	300 observations
2 .M.1	Observations	10 Targets, 2 observations	
3 .M.1	Observations	100 Targets, 1 observation	
4 .M.1	Observations	7 Targets, 2-4 observations	
5 .M.1	Observations	7 Targets, 2-4 observations	
6 .M.1	Observations	Observe when able	
1-6 .M.2	Mission Lifetime	3 Years	3-5 Years
1-6 .K.1	Laser Reference Beam	100 fW/cm ²	850 pW/cm ²
1-6 .K.2	Reference Laser Divergence	≤ 1'	14"
1-6 .K.3	Reference Laser Pointing Accuracy	7"	2"
1-6 .K.4	Reference Laser Power	0.5 - 15 W	0.5 - 15 W
1 .K.5	Instrument	KPIC/HISPEC	
2 .K.5	Instrument	UV/VIS/NIR IFU	
3 .K.5	Instrument	UV/NIR	
4 .K.5	Instrument	VIS/NIR Spectrograph	
5 .K.5	Instrument	VIS/NIR Spectrograph	
6 .K.5	Instrument	OSIRIS/LIGER	
1-6 .K.6	Time to Acquire ORCAS Laser	≤ 3 Hours	15 Minutes
1-6 .K.7	Wavefront Error Input (Zenith Angle ≤ [30°, 50°])	≤ [150nm, 160nm]	
1-6 .K.8	Tip-Tilt Error (Zenith Angle ≤ [30°, 50°])	≤ [5mas, 7mas]	
1,3-5 .L.1	AO Source Brightness	5 Magnitude	0-5 Magnitude
2 .L.1	AO Source Brightness		1 Magnitude
1-5 .L.2	Payload Used	Laser 532 nm or 1064 nm	532 / 1064 nm
6 .L.2	Payload Used	Flux Calibrator	
1-6 .L.3	Laser FOV	4' x 4'	8' x 16'
1-6 .L.4	Laser Volume	≤ 6U	4U
1-6 .L.5	Laser Mass	≤ 6kg	4kg
1-6 .L.6	Laser Power	≤ 150W	75 - 130W
1-6 .L.7	Laser Pointing	≤ 2"	0.2"
6 .F.1	Flux Calibrator	0.35-2.3 μm	
6 .F.2	Flux Calibrator Brightness	8-15 Mag	
5 .F.3	Flux Calibrator Flux Knowledge	Monitor exit flux vs wavelength slope to between than 0.4%, with a goal of 0.4%, RMS between wavelengths to 0.3%, absolute to 0.3% all wrt NIST over 0.35–2.3 μm	
5 .F.4	Flux Calibrator Appearance	≤ 0.5 arcsec Full Width Half Max	
5 .F.5	Flux Calibrator Output Scan	1° scan range; 2m resolution at receiver	
1-5 .F.6	Flux Calibrator Volume	≤ 12U	12U
1-5 .F.7	Flux Calibrator Mass	≤ 25kg	20kg
1-5 .F.8	Flux Calibrator Power	≤ 250W	200W
1-4 .S.1	Absolute Position Knowledge (GPS)	≤ 100 mas	50 mas at 3σ
1-4 .S.2	Trajectory Knowledge (GPS)	≤ 5 mas	3 mas at 3σ
1-5 .S.3	Spacecraft Body Pointing	3'	7"
1-5 .S.4	Delta-V (m/s)	≥ 4000	4200-4700
1-5 .S.5	Thrust	≥ 60 mN	100 mN
1-5 .S.6	Projected Thrust Lifetime	≥ 1000 kN-s	1200 kN-s
1-5 .S.7	Power	≥ 1600W	2300W

3 Observational Requirements

Using a ground-based observatory to make observations with ORCAS sets several requirements on when observations can take place. These requirements are defined below, and together were used to determine the times of night that each given target may be observed on a desired observation date.

First, observations must be taken at times when the sun is more than 18 degrees below the horizon. This ensures that observations will be at night, and roughly corresponds to a local solar time of 7:30 PM to 4:30 AM. The telescope shall be pointed within 60° of the local zenith angle. This corresponds to an air mass of less than 2. As the angle between the telescope pointing vector and the local zenith angle increases, the amount of atmospheric distortion increases due to the higher air mass. The angle between the pointing vector to the sun and the Earth-pointing plane of the spacecraft must be less than or equal to 89° . Finally, the angle between the Earth-pointing plane of the spacecraft and the spacecraft/observatory line of sight must be deflected up to 40° . This reduces glare from the spacecraft and will result in better images.

In order to use these requirements to map the observable sky, we pre-compute each target's maximum achievable observation duration times and expected zenith angle range for each day of the year. The map of maximum observation time can be seen in Figure 3. The contoured region corresponds to the integrated area under a spherical sector rotating around the Earth at night with a region of forbidden spacecraft positions removed. A detailed analysis on how the observable sky is built has also previously been described.¹¹

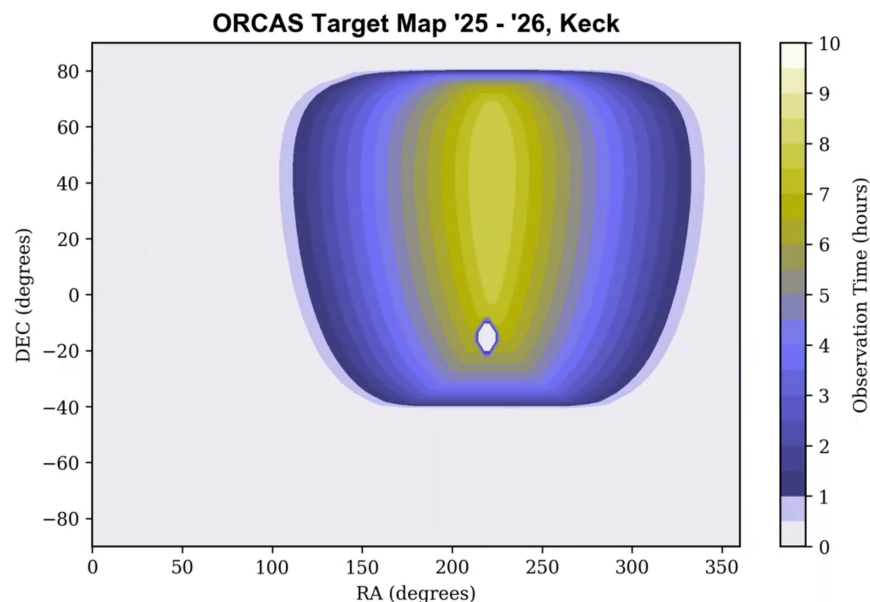


Fig 3 The Observable Sky for ORCAS working with WMKO on a night in June, contoured according to available observation time for each possible celestial coordinate. Each location in this map requires a different orbit choice to achieve the astro-stationary condition.

4 Single Observation Mission Operation Concept

4.1 Orbital Configuration

We have developed a family of orbits that can meet the ORCAS mission requirements.¹² These are five-day, highly elliptical orbits, and AO observations can be made at up to three locations near apogee. This orbit concept can be seen in Figure 4.

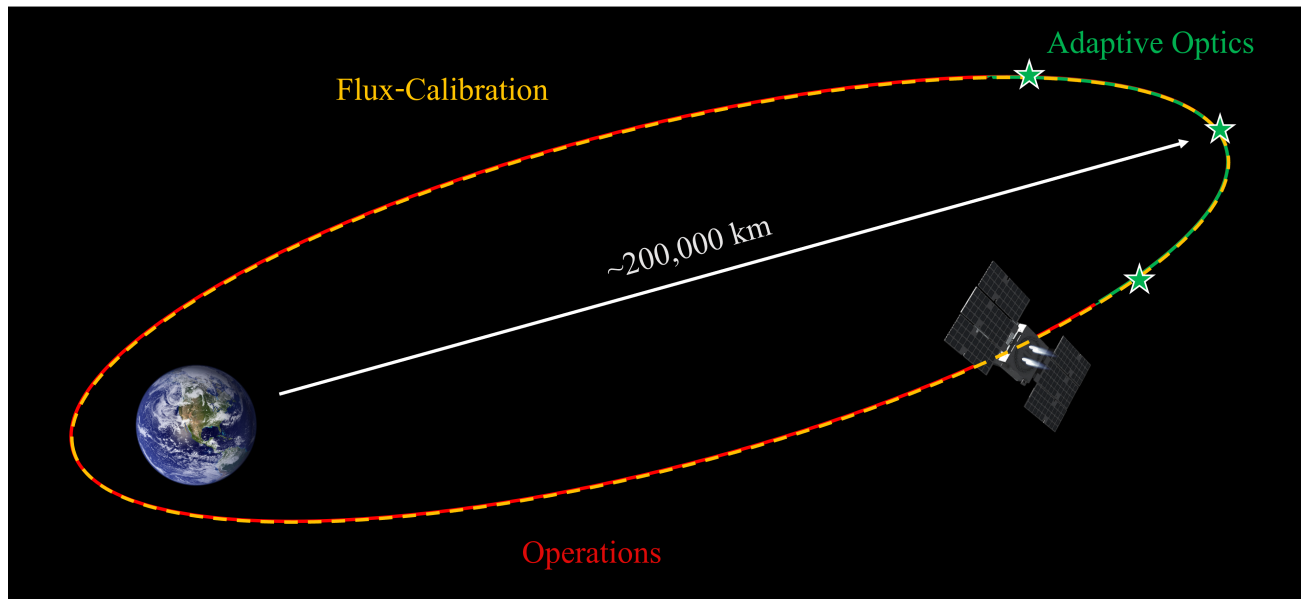


Fig 4 ORCAS concept orbit, showing when AO and flux calibration observations can be made, as well as when operations can be done on the spacecraft.

As shown, AO observations can be made at three points along the orbit close to apogee. The orbit is designed for the target at the first of these observations, and that target will have the longest observation time. The observation time itself depends on both the target declination, with declinations closer to zero corresponding to longer times, and on the wavelength of the astronomical image being taken. The field of view the telescope employs is based on the wavelength, and a larger field of view radius will correspond to a longer observation time. All three AO points on the orbit path have observation times of at least ten minutes.

Flux calibration observations can be made throughout the orbit, since they can be done based on the streaking spacecraft and do not have a minimum time requirement. Operations on the spacecraft and at WMKO can be done at any time before the AO observations, and are described more in-depth in the next section.

4.2 Mission Operations Sequence

ORCAS provides two observation modes in support of its mission science goals, AO and flux calibration, provided by the laser and the flux calibrator payloads respectively. In this section we briefly discuss the established operation sequences for each mode, which describe the chronological order of all operational steps to be taken for an observation.

Both observation modes share basic observational preparation activities as described in Table 2 that begin as the ORCAS spacecraft is near perigee. Note that this table lists optional sequences which can be done if enough time is available but are not required for every observation. Many of the steps may occur in parallel. The time listed in the tables gives a rough estimate for when the events should take place. The WMKO telescopes will be doing other observations during most of the preparations.

Table 2 The chronological sequence of actions ORCAS can perform in preparation for either observation mode and the time at which the actions can be done. Red items are for the spacecraft and blue items are for the observatory.

Operational Actions	Time
Orbit determination	T-2.5 Days
GPS sampling rate 1Hz (near perigee sub-meter accuracy)	T-2.5 Days
Mission verify targets scheduling sequence, send to WMKO	T-2.5 Days
AO Observation / Flux Calibration Prep	T-2 Days
Small maneuver corrections 1 day window	T-2 Days
Establish WMKO observation configuration, including instrument wavefront sensor, (visible/infrared), laser guide star power and divergence	T-1 Day
RF ranging - S&X band sampling at 1Hz	T-12 Hours
Test payload system readiness	T-12 Hours
Go/Nogo decision window	T-12 Hours

In Table 3, we detail the AO mode operations sequence. For a given observation, the ORCAS observing time, science target, AO science instrument and modes to be used, science ADC, and AO wavefront sensor would be prescheduled. The WMKO telescope would slew to ORCAS at a pre-determined time in advance of ORCAS being within a prescribed distance from the science target. ORCAS would lock on the WMKO laser and project either the laser wavelength toward the WMKO telescope. The appropriate AO wavefront sensor would be positioned to acquire the laser at the detected location on the AO acquisition camera. The AO wavefront sensor would remain fixed, and ORCAS position changes would be absorbed by the AO tip-tilt mirror which would be periodically offloaded to the WMKO telescope pointing. Science exposures can then be taken.

Table 4 covers the operations sequence required for flux calibration observations. When the flux calibration payload is used near an astro-stationary point, the spacecraft operations timeline needed by any WMKO AO observations will first be established (see Table 3). The required steps for an observation begin at T-30 minutes. ORCAS will provide updates with the current location and anticipated trajectory during observation to the observatory thirty minutes prior to the start of observation. The ORCAS flux calibration payload exit beam will point towards the ground-based telescope twenty minutes before observation, and at the same time ORCAS will prepare the requested light sources.

The transfer from one observation orbit to the next will take between 0 and 20 days. The spacecraft will have four thrusters for a total of 100 mN of available thrust. Figure 5 shows an example transfer orbit going from an initial target to a final target one degree of right ascension away the initial one. As shown, a series of small thrusts will be done to move into the next orbit. In total, changing the target by one degree in either direction costs 30m/s of fuel. The orbit shown has a transfer time of one orbit period, or five days, but transfers between significantly different orbits could take longer. Repeat observations will not have any transfer time at all, so we used an average transfer time of five days.

Table 3 Time stamped AO operations sequence. Red items are for the spacecraft and blue items are for the observatory.

AO Observation Sequence	Time
Projected vs. measured trajectory comparison to ground	T-3 Hours
WMKO system configuration (AO, wavefront sensor, instrument)	T-3 Hours
Fine maneuver corrections (1 hour window)	T-3 Hours
ORCAS establishes communication with mission ops center to sync ops with WMKO	T-3 Hours
Mission and science ops centers provide location to WMKO	T-2 Hours
WMKO acquires science field location and centers (point telescope to ORCAS)	T-1.8 Hours
WMKO - Detuned Laser Guide Star (LGS) (ground) projected toward science target	T-1.7 Hours
ORCAS body points laser payload FOV to the LGS beam	T-1.6 Hours
ORCAS laser payload acquires LGS (point to target, search pattern if not seen)	T-1.3 Hours
ORCAS laser payload locks and provides to required beam	T-1.2 Hours
Safety gap (second attempt to acquire if required)	T-1.2-0.5 Hours
WMKO AO system sets predetermined ORCAS power and wavelength, closes WMKO AO loops and tracks ORCAS source	T-0.5 Hours
Flight dynamics provides WMKO, mission and science operations centers an updated ORCAS trajectory estimate (GPS + Optimetrics)	T-0.25 Hours
Begin AO Observation #1	T
End AO Observation #1	T + Δ T (minutes - hours)
Total Time	2-3 Hours

Table 4 Time stamped operations sequence for flux calibration. Red items are for the spacecraft and blue items are for the observatory.

Flux Calibration Observation Sequence	Time
ORCAS updates with current location and anticipated trajectory to ground-based telescope	T – 30 minutes
ORCAS body points the flux calibration payload exit beam towards ground-based telescope	T – 20 minutes
ORCAS prepares requested light sources	T – 20 minutes
ORCAS activates one wavelength to ground-based telescope can confirm tracking & guiding (if desired)	T – 10 minutes
Begin observation	T minutes
End observation	T + Δ T minutes
Total Time	30 minutes

Based on these observation sequences and the described transfer orbits, a sample sequence which outlines the proposed mission timeline is given in Table 5. The mission starts out with the spacecraft's release from the rideshare spacecraft and a series of maneuvers to get it into the proposed orbit. The spacecraft will be in position about 6.5 months after launch. At that point, observations can begin. Each orbit has a period of five days. During this time, three AO observations can be made, and flux calibration observations can be made any other time. The transfer to the next orbit will take 0 to 20 days, depending on the difference in orbits. The total observation sequence therefore is on average about 10 days, which assumes one intermediate 'buffer' orbit between each reconfiguration and subsequent observations. This sequence will be repeated about 100 times to allow for observations of as many targets as possible. Once the mission is finished, de-orbit will take 120 days.

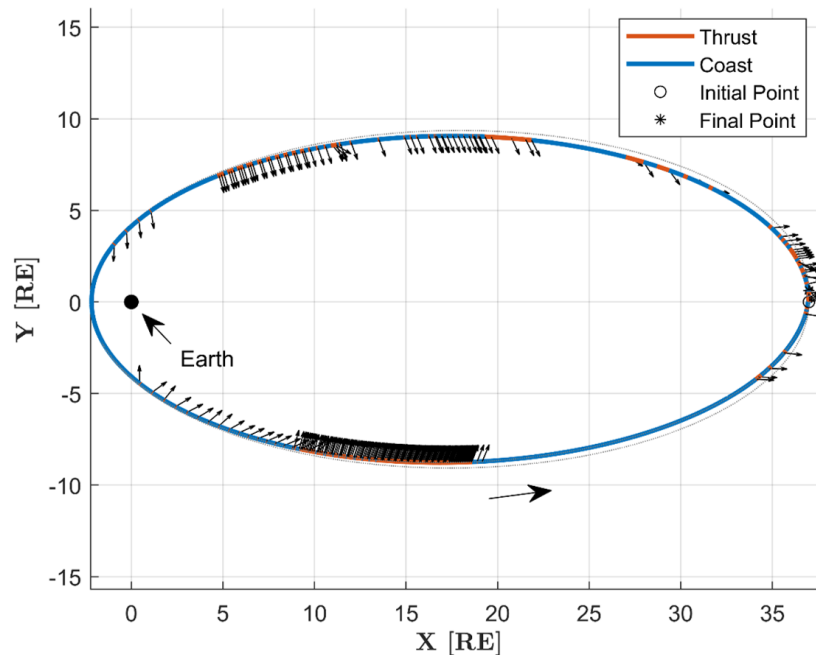


Fig 5 An example transfer orbit resulting in one degree of right ascension change is shown. This transfer orbit would take 30m/s of fuel and 5 days to complete.

Table 5 Mission Timeline
Sample Mission Sequence

Commissioning	Release spacecraft Maneuver to science orbit	6.5 Months
Science (Single Observation Orbit)	Orbit Determination, Verify target schedule at WMKO AO Observation Prep	2.5 Days 3 Hours
	Observation #1 - Imaging Drift to next observation point	3 Hours 21 Hours
	Observation #2 - IFU Drift to next observation point	3 Hours 21 Hours
	Observation #3 - Imaging Flux Calibration	3 Hours 3 Hours
	Transfer to next science orbit - will be done about every 2 orbits to allow repeat observations	5-20 Days
	Total time for 1 observation sequence	10 Days
Total Science Lifetime	Repeat 10-day observation sequence (3 AO observations each) up to 110 times	3 years
End-of-Life	De-Orbit and Disposal	120 Days

5 Methodology

Based on the previous section, each observation will take an average of 10 days, and over 100 such observations can be performed over the mission lifetime. We also use several parameters defined in Section 2 of this report to determine the remaining parameters. We used the value of 4200-4700 m/s of

fuel based on requirement 1-6.M.2 in the requirements, but subtracted 700 m/s allotted to consumption during the cislunar drop-down, leaving 4000 m/s. Additionally, we assumed a 3-year mission starting December 1st, 2025 based on requirement 1-5.S.4.

Transferring between targets is, at a basic level, the process of re-configuring to a new orbit in the ORCAS HEO family which is designed for the desired observation target. As informed by collocation-optimized low thrust orbital reconfiguration simulations, we find that the propellant cost of inter-target transfers can be upper-bounded in direct proportion to the angular distance between targets, approximately 30 m/sec/deg, and approximately extended to large transfers by dividing it into the smallest achievable number of intermediate orbits. With estimates of each possible target's value, conditions of observation and the costs of traversing between them in hand, it is possible to optimize the mission profile for maximum delivered value within its required operational constraints, lifetime and propellant.

We have developed a metaheuristic (genetic) algorithm to explore and optimize this very high dimensional time dependent travelling salesman problem over a range of future and current scientific objectives and engineering constraints. An overview of this optimization method is provided in Figure 6. A detailed presentation has previously been given.^{13,14}

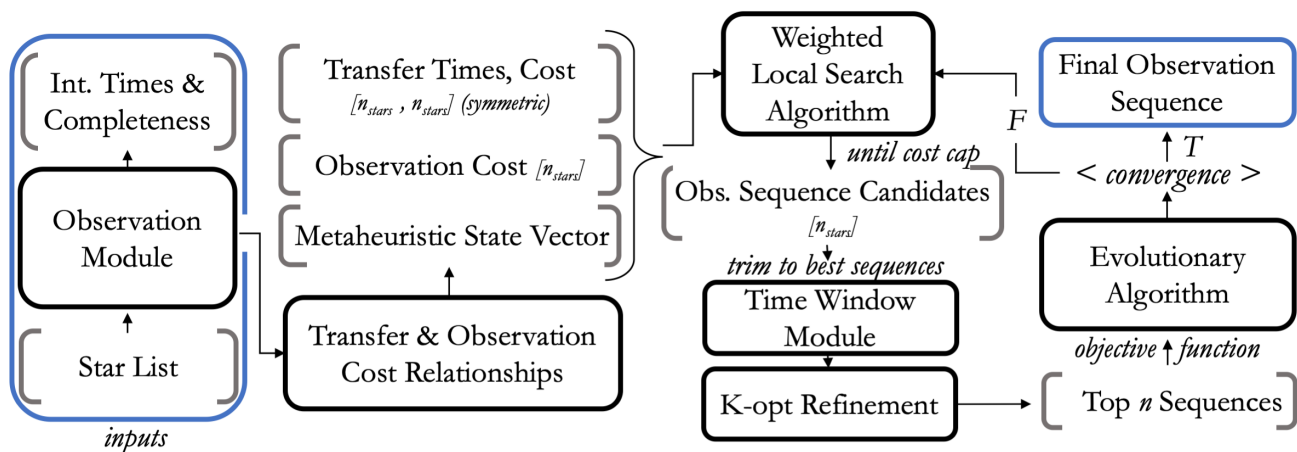


Fig 6 Sequence-Optimizing algorithm flowchart.

To prioritize interesting targets, we scale their relative value — on top of their observability and, in the case of exoplanets, expected completeness — by a combined weight of uniqueness in the target list data-set and a heuristic ‘desirability’ factor informed by mission science cases. For instance, M87 is considered valuable. Regions such as the HDF or XMM-LSS are modelled by a discrete set of between 6-10 observation ‘targets’ over their surface. We do not include solar system bodies at this stage, but work is ongoing to include them; we expect many observation opportunities for targets near the ecliptic.

6 Results

A unique sequence using our schedule optimization code has been generated for a scientific target priority scenario, as presented below. Figure 7 illustrates the motion of ORCAS across the sky as it performs observations throughout the first half of the mission lifetime.

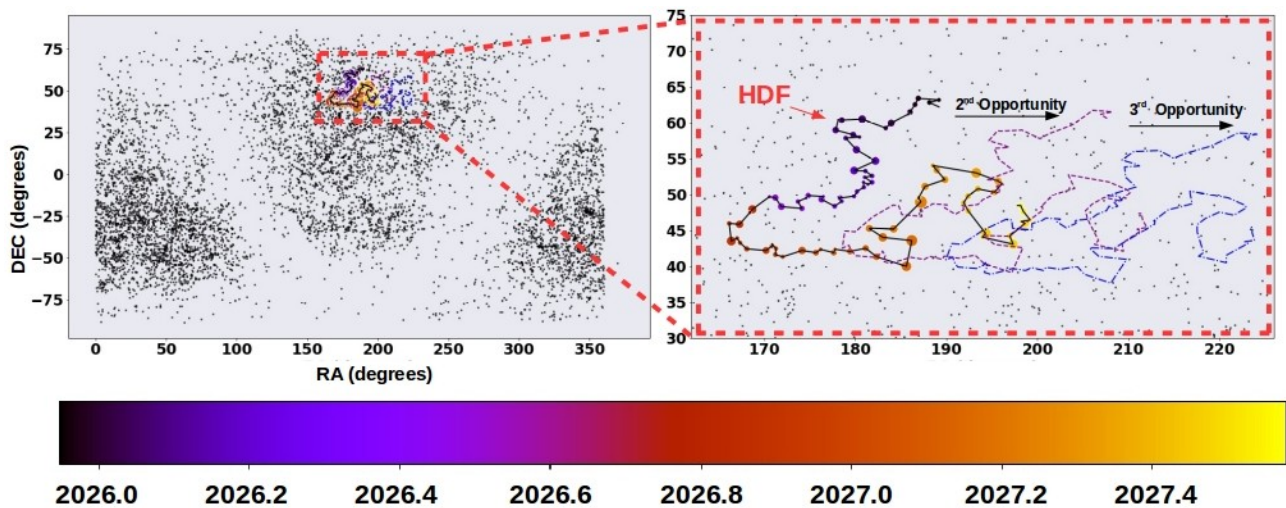


Fig 7 Targets with ORCAS across the first half of a 3-year mission lifetime. The size of each observation corresponds to the total cost to observe, and the color corresponds to the time (in years) that has already passed. In total, there are 285 AO observations in this sequence containing the Hubble Deep Field and spread across 2 additional observing opportunities as seen in the purple and blue curves. This sequence serves only as an example and not as a final mission observing schedule.

Figure 7 shows both the primary observation that each orbit is designed for, and the second and third AO observation opportunities. Each primary target is allocated two observation orbits. The second and third AO observation opportunities fall on the nights at and following apogee and move across a stretch of sky approximately $\pm 10^\circ$ RA from the original target. Work is ongoing to identify the fraction of these secondary observation opportunities which can be made on targets in our list. In general we find that more heterogeneous target priorities reduce the total number of optimal target list observations, as they produce a mission profile that stretches over a larger range of sky in reaching ‘desirable’ targets.

As seen in Figure 7, ORCAS can perform about 300 AO observations over the mission lifetime. Table 6 provides the coordinates of all ORCAS AO target opportunities and the dates each observation will occur. It is important to remember that each science orbit will contain three AO observation opportunities, so consecutive targets within 24 hours will contain large jumps in Right Ascension (RA) but very small differences in Declination (DEC). The table does not provide the names of each target because it is only here to serve as an example of what the mission schedule can do. In future versions, all potential targets will have a different priority value that will reflect how the schedule is built.

Table 6 The observation schedule built within the ORCAS mission schedule optimization tool.

Observation	RA	DEC	Retargeting (m/s)	Date	Observation	RA	DEC	Retargeting (m/s)	Date	Observation	RA	DEC	Retargeting (m/s)	Date
1	189.205	62.22	0.0	2025-12-08	92	203.1798	45.3641	0.0	2026-05-19	184	198.4295	42.6033	0.0	2027-03-05
2	189.205	62.22	0.0	2025-12-13	93	176.3	49.33	40.313	2026-05-22	185	209.8117	40.9724	nan	2027-03-06
3	188.15	62.83	23.41	2025-12-18	94	189.8009	48.1839	0.0	2026-05-23	186	183.025	44.0389	70.348	2027-03-09
4	206.9664	61.1933	0.0	2025-12-19	95	202.159	46.2307	0.0	2026-05-24	187	195.3279	43.0413	0.0	2027-03-10
5	189.2	63.19	17.922	2025-12-23	96	176.5	49.73	12.617	2026-05-27	188	206.7781	41.3872	0.0	2027-03-11
6	208.2306	61.5365	0.0	2025-12-24	97	190.1056	48.5719	0.0	2026-05-28	189	181.55	45.2836	48.84	2027-03-14
7	186.93	63.41	31.303	2025-12-28	98	202.5408	46.5937	0.0	2026-05-29	190	194.106	44.2523	0.0	2027-03-15
8	206.0948	61.7461	0.0	2025-12-29	99	174.83	49.87	32.614	2026-06-01	191	205.7524	42.5329	0.0	2027-03-16
9	222.0786	58.5936	0.0	2025-12-30	100	188.4729	48.708	0.0	2026-06-02	192	181.5561	45.3337	1.57	2027-03-19
10	186.57	62.55	26.261	2026-01-02	101	200.9351	46.7204	0.0	2026-06-03	193	194.1226	44.3011	0.0	2027-03-20
11	205.2232	60.9262	0.0	2026-01-03	102	174.6	49.52	11.416	2026-06-06	194	205.7771	42.5789	0.0	2027-03-21
12	220.9259	57.8722	0.0	2026-01-04	103	188.1505	48.3685	0.0	2026-06-07	195	184.22	45.22	56.338	2027-03-24
13	186.02	61.5	32.436	2026-01-07	104	200.5447	46.4029	0.0	2026-06-08	196	196.7628	44.1902	0.0	2027-03-25
14	204.0893	59.9232	0.0	2026-01-08	105	173.7	49.03	22.939	2026-06-11	197	208.3988	42.4744	0.0	2027-03-26
15	219.4602	56.9833	0.0	2026-01-09	106	187.1235	47.8928	0.0	2026-06-12	198	187.2154	48.9671	127.956	2027-03-31
16	185.83	61.21	9.117	2026-01-12	107	199.4248	45.9579	0.0	2026-06-13	199	200.6231	47.8316	0.0	2027-04-01
17	203.7455	59.6461	0.0	2026-01-13	108	174.15	48.07	30.151	2026-06-16	200	212.9124	45.9008	0.0	2027-04-02
18	219.0262	56.7362	0.0	2026-01-14	109	187.335	46.9605	0.0	2026-06-17	201	186.9817	49.5489	18.05	2027-04-05
19	183.95	59.97	46.372	2026-01-17	110	199.4585	45.0839	0.0	2026-06-18	202	200.5397	48.3965	0.0	2027-04-06
20	201.2398	58.4582	0.0	2026-01-18	111	171.88	48.32	46.002	2026-06-21	203	212.9394	46.4295	0.0	2027-04-07
21	16.1477	55.6738	0.0	2026-01-19	112	185.1261	47.2036	0.0	2026-06-22	204	186.9	49.43	3.937	2027-04-10
22	213.35	59.27	22.893	2026-01-22	113	197.2947	45.3119	0.0	2026-06-23	205	200.4266	48.281	0.0	2027-04-11
23	200.3086	57.7865	0.0	2026-01-23	114	171.2238	49.5698	39.657	2026-06-26	206	212.804	46.3214	0.0	2027-04-12
24	215.0134	55.0696	0.0	2026-01-24	115	184.7872	48.4167	0.0	2026-06-27	207	187.6679	51.1373	53.296	2027-04-15
25	180.7646	60.522	54.07	2026-01-27	116	197.191	46.4483	0.0	2026-06-28	208	201.6607	49.9369	0.0	2027-04-16
26	198.3265	58.9873	0.0	2026-01-28	117	170.57	49.7	13.27	2026-07-01	209	214.3773	47.8668	0.0	2027-04-17
27	213.3983	56.148	0.0	2026-01-29	118	184.1677	48.5429	0.0	2026-07-02	210	189.85	52.08	49.52	2027-04-20
28	178.5183	60.3733	33.53	2026-02-01	119	196.5971	46.5665	0.0	2026-07-03	211	204.1192	50.8498	0.0	2027-04-21
29	196.0058	58.8447	0.0	2026-02-02	120	168.6859	47.936	64.695	2026-11-08	212	217.0342	48.7162	0.0	2027-04-22
30	211.033	56.0206	0.0	2026-02-03	121	168.43	47.5	14.069	2026-11-13	213	188.95	53.4	42.842	2027-04-25
31	178.13	60.42	5.905	2026-02-06	122	167.291	45.8571	54.579	2026-11-18	214	203.6315	52.1275	0.0	2027-04-26
32	195.6404	58.8894	0.0	2026-02-07	123	179.9694	44.8101	0.0	2026-11-19	215	216.8368	49.8998	0.0	2027-04-27
33	210.6822	56.0606	0.0	2026-02-08	124	166.1529	45.9853	24.056	2026-11-23	216	188.53	54.05	20.882	2027-04-30
34	177.8525	58.9884	43.149	2026-02-11	125	178.8591	44.9347	0.0	2026-11-24	217	203.426	52.7561	0.0	2027-05-01
35	194.6819	57.516	0.0	2026-02-12	126	166.3787	43.5216	74.064	2026-11-28	218	216.7811	50.4801	0.0	2027-05-02
36	209.3065	54.826	0.0	2026-02-13	127	178.5806	42.5376	0.0	2026-11-29	219	193.2996	53.02	90.46	2027-05-06
37	179.7737	58.3432	35.678	2026-02-16	128	189.9527	40.9102	0.0	2026-11-30	220	207.8592	51.7597	0.0	2027-05-07
38	196.316	56.8958	0.0	2026-02-17	129	167.02	43.93	18.522	2026-12-03	221	220.9797	49.5597	0.0	2027-05-08
39	210.7601	54.2653	0.0	2026-02-18	130	179.3015	42.9353	0.0	2026-12-04	222	195.7	51.88	55.637	2027-05-11
40	180.48	58.02	14.777	2026-02-21	131	190.7351	41.2868	0.0	2026-12-05	223	209.9091	50.6563	0.0	2027-05-12
41	196.8826	56.5848	0.0	2026-02-22	132	167.35	43.27	21.05	2026-12-08	224	222.7816	48.5362	0.0	2027-05-13
42	211.2387	53.9836	0.0	2026-02-23	133	179.5039	42.2927	0.0	2026-12-09	225	196.12	51.5	13.817	2027-05-16
43	178.95	57.87	24.77	2026-02-26	134	190.8385	40.6779	0.0	2026-12-10	226	210.2174	50.2881	0.0	2027-05-17
44	195.289	56.4406	0.0	2026-02-27	135	168.08	42.43	29.881	2026-12-13	227	223.0092	48.194	0.0	2027-05-18
45	209.6036	53.8527	0.0	2026-02-28	136	180.0778	41.4746	0.0	2026-12-14	228	195.3	50.32	38.649	2027-05-21
46	180.13	56.25	52.271	2026-03-03	137	191.2898	39.9016	0.0	2026-12-15	229	209.0643	49.1443	0.0	2027-05-22
47	195.8167	54.8803	0.0	2026-03-04	138	170.2	42.2039	47.516	2026-12-18	230	221.6152	47.1282	0.0	2027-05-23
48	209.7061	52.4308	0.0	2026-03-05	139	182.1569	41.2544	0.0	2026-12-19	231	193.48	50.8	37.554	2027-05-26
49	182.2258	54.6995	58.588	2026-03-08	140	193.3366	39.6924	0.0	2026-12-20	232	207.3774	49.61	0.0	2027-05-27
50	197.3449	53.3837	0.0	2026-03-09	141	170.85	42.83	23.65	2026-12-23	233	220.025	47.5623	0.0	2027-05-28
51	210.8523	51.0854	0.0	2026-03-10	142	182.9215	41.864	0.0	2026-12-24	234	192.4	49.82	35.953	2027-05-31
52	179.8762	53.3488	57.926	2026-03-13	143	194.1912	40.2714	0.0	2026-12-25	235	206.0296	48.6596	0.0	2027-06-01
53	194.5413	52.0781	0.0	2026-03-14	144	170.87	43.1	8.094	2026-12-28	236	218.4821	46.6752	0.0	2027-06-02
54	207.7351	49.8541	0.0	2026-03-15	145	182.9919	42.1269	0.0	2026-12-29	237	191.92	48.87	30.004	2027-06-05
55	181.12	53.28	22.38	2026-03-18	146	194.3012	40.5209	0.0	2026-12-30	238	205.3031	47.7374	0.0	2027-06-06
56	195.7626	52.0114	0.0	2026-03-19	147	171.3	42.48	20.865	2027-01-02	239	217.5737	45.8125	0.0	2027-06-07
57	208.9413	49.7924	0.0	2026-03-20	148	183.307	41.5231	0.0	2027-01-03	240	192.42	47.72	35.914	2027-06-10
58	181.85	52.6	24.296	2026-03-23	149	194.5261	39.9478	0.0	2027-01-04	241	205.5211	46.6209	0.0	2027-06-11
59	196.2778	51.3535	0.0	2026-03-24	150	171.22	41.63	25.568	2027-01-07	242	217.5812	44.7644	0.0	2027-06-12
60	209.3056	49.1832	nan	2026-03-25	151	183.0753	40.6954	0.0	2027-01-08	243	194.3202	44.6071	101.382	2027-06-16
61	181.03	52.42	15.902	2026-03-28	152	194.1742	39.1608	0.0	2027-01-09	244	206.7368	43.5942	0.0	2027-06-17
62	195.4026	51.1793	0.0	2026-03-29	153	172.03	41.33	20.317	2027-01-12	245	218.2749	41.9108	0.0	2027-06-18
63	208.3907	49.0215	0.0	2026-03-30	154	183.8332	40.403	0.0	2027-01-13	246	193.97	44.07	17.784	2027-06-21
64	181.8513	51.7143	26.032	2026-04-02	155	194.8908	38.8827	0.0	2027-01-14	247	206.2791	43.0716	0.0	2027-06-22
65	196.0116	50.4959	0.0	2026-04-03	156	174.1608	42.2097	54.489	2027-01-17	248	217.734	41.4158	0.0	2027-06-23
66	208.8485	48.3872	0.0	2026-04-04	157	186.1187	41.26	0.0	2027-01-18	249	197.3562	43.0848	79.301	2027-06-26
67	181.4	51.42	12.191	2026-04-07	158	197.2993	39.6977	0.0	2027-01-19	250	209.4753	42.1121	0.0	2027-06-27
68	195.4742	50.2108	0.0	2026-04-08	159	175.68	41.9	35.091	2027-01-22	251	220.7824	40.5069	0.0	2027-06-28
69	208.2494	48.1218	0.0	2026-04-09	160	187.5825	40.9583	0.0	2027-01-23	252	196.975	44.2167	34.95	2027-07-01
70	180.9	51.73	13.164	2026-04-12	161	198.7194	39.411	0.0	2027-01-24	253	209.3131	43.2143	0.0	2027-07-02
71	195.0649	50.511	0.0	2026-04-13	162	176.2	42.35	17.784	2027-01-27	254	220.7907	41.551	0.0	2027-07-03
72	207.905	48.4013	0.0	2026-04-14										

6.1 Sensitivity

The ORCAS mission concept may change in the future due to the evolution of science requirements and engineering capabilities. Therefore, this section discusses how these delivered target sequences are sensitive to uncertainty and how the number of observations may change with changes to the retargeting fuel cost and orbit transfer time. In Figure 8, we generate optimized mission profiles with varying re-targeting costs and times by multiplying their respective cost functions by factors between 0.5 and 2.0. We developed a two-dimensional space where each point has an optimal target sequence. In terms of propellant consumption, the inverse of our cost factor effectively reflects a changed total fuel allocation. For instance 1.2x Delta-V costs corresponds to approximately 83% tank size.

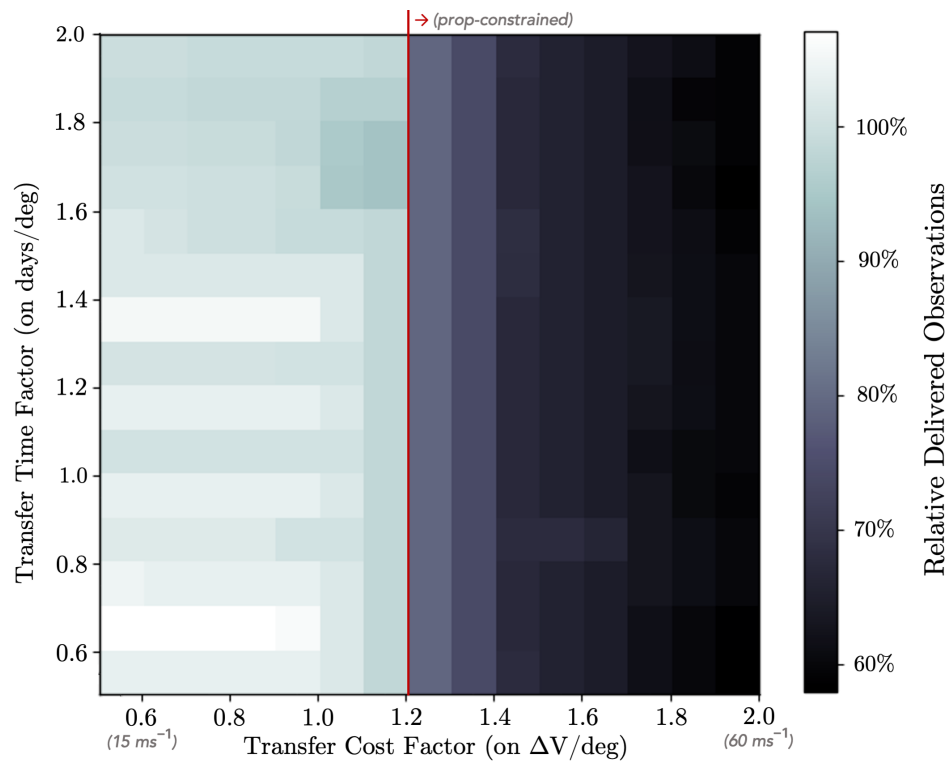


Fig 8 Sensitivity map of delivered observations to time and fuel over a mission lifetime, plotted relative to scaled transfer times and Delta-V costs.

As shown, target delivery is most sensitive to the transfer fuel cost, and the mission becomes propellant-constrained at only 1.2x the current costs. The impact is about 60% target delivery for a doubled fuel cost, and about 95% target delivery for a doubled transfer time.

In addition to changes to the transfer time and fuel costs, other changes to the mission could change the target delivery. Because the current method involves optimizing only for the first AO observation in an orbit, some of the second and third orbits could fall on locations of the sky where there is no interesting target, resulting in lost observation opportunities. Regions of the sky with a lower density of important astronomical objects could result in longer transfer times and higher fuel costs to get from orbit to orbit or a decrease in useful observation opportunities. Weather effects could also play a role; however, it should be noted that in the case of bad weather at the time of an observation the orbit could simply be repeated by maintaining the orbit. This would result in minimal use of fuel to recover the

observation. Additionally, Mauna Kea in general has 76% clear nights every year, so the majority of observations would be successful.

7 Discussion and Future Work

In this paper, we have presented a highly elliptical orbit which can meet AO observation requirements and a tool which can be used to optimize the order of observation targets viewed. We show that over the ORCAS mission lifetime of 3 years and with a fuel budget of 4000 m/s, 300 AO observations can be made. Additionally, since flux calibration observations can be made throughout the orbit, over 1,500 flux calibration observations can be made within the mission lifetime. We present an example sequence of observation targets which can be viewed. The tool can be used in real-time during the mission to update the order of observations based on the importance of various targets and also based on weather events or nights with low visibility.

This method is based on making three AO observations in a single elliptical orbit, and currently only takes the first target into account during the optimization process. Future work should include updating the model to consider the observation time and position of all the target observations. Additionally, this type of astrostationary orbit has also been considered for other missions, including a remote occulter which would orbit the Earth and inertially align with ground based observatories to improve images of the exoplanets.^{15,16} This mission planning tool could be adapted for use in that mission.

8 Bibliography

References

- 1 O. Guyon, “Limits of Adaptive Optics for High-Contrast Imaging,” *The Astrophysical Journal* **629**, 592–614 (2005).
- 2 D. Mawet, L. Pueyo, P. Lawson, *et al.*, “Review of small-angle coronagraphic techniques in the wake of ground-based second-generation adaptive optics systems,” in *Space Telescopes and Instrumentation 2012: Optical, Infrared, and Millimeter Wave*, M. C. Clampin, G. G. Fazio, H. A. MacEwen, *et al.*, Eds., **8442**, 62 – 82, International Society for Optics and Photonics, SPIE (2012).
- 3 P. Wizinowich, D. Mignant, A. Bouchez, *et al.*, “The w. m. keck observatory laser guide star adaptive optics system: Overview,” **118**(297-309) (2006).
- 4 “Astro2020: Decadal survey on astronomy and astrophysics,” in *Bulletin of the American Astronomical Society, APC white papers, no. 284* **51** (2019).
- 5 N. R. Council, *New Worlds, New Horizons in Astronomy and Astrophysics*, The National Academies Press, Washington DC (2010). [doi:10.17226/12951].
- 6 T. L. Team, “The LUVOR Mission Concept Study Final Report,” *arXiv:1912.06219 [astro-ph]* (2019).
- 7 ESO, “The E-ELT Construction Proposal.” https://www.eso.org/sci/facilities/eelt/docs/e-elt_constproposal.pdf (2011).
- 8 G. H. Sanders, “The Thirty Meter Telescope (TMT): An International Observatory,” *Journal of Astrophysics and Astronomy* **34**, 81–86 (2013).

- 9 B. S. Gaudi, S. Seager, B. Mennesson, *et al.*, “The habitable exoplanet observatory (habex) mission concept study final report,” (2020). arXiv:2001.06683v2.
- 10 E. Peretz, K. McCormick, E. Moehring, *et al.*, “Orbiting configurable artificial star multi-wavelength payload,” (In preparation).
- 11 E. Peretz, J. Mather, L. Parbarcius, *et al.*, “Mapping the observable sky for a remote occulter working with ground-based telescopes,” *Journal of Astronomical Telescopes, Instruments, and Systems* **7**(1) (2021).
- 12 E. Peretz, C. Hamilton, J. Mather, *et al.*, “Astro-stationary orbits in coordination with ground based observatories for enhanced observations,” (In preparation).
- 13 E. Peretz, J. C. Mather, K. Hall, *et al.*, “Exoplanet imaging scheduling optimization for an orbiting starshade working with extremely large telescopes,” *Journal of Astronomical Telescopes, Instruments, and Systems* **7**(2) (2020).
- 14 E. Peretz, K. Hall, J. Mather, *et al.*, “Exoplanet imaging performance envelopes for starshade-based missions,” *Journal of Astronomical Telescopes, Instruments, and Systems* **7**(2) (2021).
- 15 A. W. Koenig, S. D’Amico, E. Peretz, *et al.*, “Optimal spacecraft orbit design for inertial alignment with ground telescope,” IEEE Aerospace Conference (2021).
- 16 J. C. Mather, E. Peretz, J. Arenberg, *et al.*, “Orbiting starshade to observe exoplanets with ground-based telescopes (in review),” *Nature Astronomy* (2021).